American Mineralogist, Volume 100, pages 1595–1599, 2015

Dissolved Cl, oxygen fugacity, and their effects on Fe behavior in a hydrous rhyodacitic melt

Aaron S. Bell[1,*] and James D. Webster[2]

[1]Institute of Meteoritics, University of New Mexico, Albuquerque, New Mexico 87109, U.S.A.
[2]Department of Earth and Planetary Science, American Museum of Natural History, New York, New York 10024, U.S.A.

Abstract

We have conducted a series of experiments to evaluate the intrinsic effects of dissolved chlorine on $Fe^{3+}/\Sigma Fe$ and magnetite solubility in hydrous chloride-rich rhyodaciticliquids. The addition of Cl to the melt appears to have two prominent effects on iron in the melt: (1) dissolved Cl appears to perturb the magnetite-melt equilibrium, such that greater FeO^{total} contents are required to support magnetite saturation in Cl-bearing melts than in Cl-free melts of equivalent bulk compositions; and (2) a systematic and progressive decrease of the measured $Fe^{3+}/\Sigma Fe$ as f_{O_2} is increased. These two intimately related effects each have important implications for redox processes occurring in Cl-enriched arc magmas.

Keywords: Iron, oxygen fugacity, chlorine, XANES

Introduction

Iron is by far the most abundant multivalent element present in terrestrial magmas (Wilke 2005) and therefore exerts a proportionally large influence on the overall redox behavior of natural silicate melts. Much analytical and experimental effort has been exerted to illuminate the relationships between the molar ratio of $FeO_{1.5}/FeO$ and intensive parameters such as bulk melt composition, pressure, and temperature (Sack et al. 1980; Killinc et al. 1983; Kress and Carmichael 1991; Tangeman et al. 2001; Ottonello et al. 2001; Jayasuriya et al. 2004; Moretti 2005; Borisov and McCammon 2010). Previous efforts have also been extended to account for the effects of dissolved volatile constituents on Fe redox behavior. Specifically, the intrinsic effects of dissolved water on the equilibrium ratio of ferric and ferrous iron have been the subject of several studies as well as the source of much debate and controversy (Moore et al. 1995; Baker and Rutherford 1996; Gaillard et al. 2001; Wilke et al. 2002). Though a considerable quantity of work has been directed toward understanding dissolved water's effects on the redox systematics of Fe, the potential effects of other volatile elements that fill anionic structural roles have only been investigated to a limited extent. After dissolved hydroxyl, chlorine is the second-most abundant anionic volatile component in evolved, subduction-related silicate magmas (Wallace 2005). Given the propensity for Cl to form ionic bonds with divalent cations in silicate melts (Carroll and Webster 1994; Webster and De Vivo 2002; Zimova and Webb 2006; Filiberto and Treiman 2009; Filiberto et al. 2014; Webb et al. 2014; Webster et al. 2015), it is reasonable to hypothesize that dissolved chlorine may exert a significant influence on redox behavior of iron. Such an effect would have important implications for the stability fields of Fe-bearing minerals in equilibrium with chlorinated melts, as well as understanding the relationship between the measured, formal valence of iron and magmatic f_{O_2}. The latter point is of considerable importance, as the formation of Fe-Cl species in the melt (i.e., the formation of a $FeCl_2$ melt component analogous to the oxide component FeO) requires that the relative concentration of Fe^{2+} in the melt is not exclusively determined by magmatic f_{O_2}, but is instead a function of both f_{O_2} and the Cl content (i.e., f_{Cl_2}) of the melt.

This initial hypothesis is supported by the data and conclusions drawn from several previous studies on Cl solubility. The pioneering work of Webster and DeVivo (2002) established a quantitative link between the concentration of divalent cations such as Mg, Fe, and Ca and melt Cl-dissolution capacity. Several studies on the effects of Cl on the viscosity of silicate melts observed that the addition of Cl to some Fe-bearing melts results in an increase in the viscosity of these liquids, suggesting that dissolved Cl bonds with Fe^{2+} in the melt and disrupts its network-modifying structural role (Dingwell and Hess 1998; Zimova and Webb 2006; Webb et al. 2014). Additionally, a recent X-ray absorption near edge structure (XANES) study conducted by Evans et al. (2008) identified dissolved Cl bonded to divalent cations in the form of Mg-Cl and Ca-Cl species in haplobasaltic glasses. Although the melts of this study did not contain Fe, the authors concluded that divalent Ca and Mg form Cl complexes with a short-range structure similar to that of crystalline $MgCl_2$ and $CaCl_2$. Given the strong similarities between the ionic radius and field strength of Fe^{2+} and Mg^{2+}, it seems probable that Fe-Cl complexes also exist as species in silicate melts. In this work we present a series of experiments designed to investigate the potential relationship between Fe and Cl in a hydrous rhyodacitic liquid. While this work in no way represents a comprehensive study of the effects of Cl on Fe in melts, the experiments presented do provide some new and unique insight into potential Fe-Cl interactions in felsic melts.

Experimental design and rationale

Two sets of experiments were conducted, each with a different purpose. The first set of experiments was designed to investigate the effect of dissolved Cl on magnetite solubility in hydrous chlorinated rhyodacitic melts at controlled f_{O_2}. Iron was added to the starting charges as a single chip of magnetite or a mixture of glass and magnetite powder that was located at one end of the capsule. These experiments were purposefully configured in this manner, so that the melt from only one end of the experimental charge would be in direct contact with magnetite. This set of experiments will be referred to as the MagLiq series.

* E-mail: asbell@unm.edu

0003-004X/15/0007–1595$05.00/DOI: http://dx.doi.org/10.2138/am-2015-5197

A second set of melt-only experiments was designed to examine the potential effects of dissolved Cl on the $Fe^{3+}/\Sigma Fe$ of the quenched rhyodacitic melts over a range of f_{O_2} values. These experiments have been designated the SRD series. In addition to the Cl-bearing experiments, a few redox-controlled experiments were performed to develop additional dacitic-glass XANES standards. Experimental conditions, Fe and Cl concentrations, and the XANES measured $Fe^{3+}/\Sigma Fe$ values for the quenched melts are presented in Table 1.

All of the SRD and MagLiq experiments were performed in 3 mm (OD) × 2.7 mm (ID) × 20 mm (length) Au capsules. At the temperatures of the experiments in this study, Au capsules are sufficiently H_2 permeable to attain redox equilibrium within the first several hours of the experiment (Gaillard et al. 2001). Water and Cl were added to the charges in the form of a Na-K-H chloride solution. Appropriate quantities (10–15 mg) of a prepared NaCl-KCl-HCl solution (ΣCl = 7.5 wt%) were added to each SRD2 capsule with a micro-pipette to ensure that each charge remained fluid-saturated throughout the duration of the experiment (each experiment contained from 30–45 mg SRD2 starting glass). The fluid-melt ratios for these experiments are somewhat variable, therefore the extent of Fe scavenging and alkali exchange have differently affected the melt composition of each experiment, albeit to a relatively limited extent. For the MagLiq runs, special care was taken to minimize the fluid-melt ratio present at run conditions to mitigate Fe loss and alkali exchange due to fluid scavenging (Bell and Simon 2011).

Experiments were conducted in a Shaw membrane-equipped internally heated pressure vessel apparatus at the American Museum of Natural History (AMNH). All experimental runs were conducted at 950 °C and pressures of either 130 or 150 MPa. Run durations for the equilibrium MagLiq and SRD experiments ranged from 132 to 212 h. Temperature and thermal gradients were measured with two factory-calibrated, Inconel-sheathed type-K thermocouples. The maximum measured thermal gradient (ΔT) over the length of an experimental capsule was ±7 °C. Pressure was measured with a bourdon tube-type strain gauge with a precision of ±10 bar. Experiments were isobarically quenched at approximately 10 °C/s.

The oxidation state of the experimental charges was controlled with a platinum-sheathed Shaw membrane that was positioned immediately adjacent to the experimental capsules. The partial pressure of H_2 transmitted from the membrane to the Ar pressure medium in the vessel was monitored with a high-precision bourdon tube gauge. Oxygen fugacities imposed by the membrane were verified with a solid-state Co-Pd-CoO redox sensor identical to those described by Taylor et al. (1992). Oxygen fugacity calculated from the redox sensor alloy composition ($Co_{39.5}Pd_{40.5}$) was $\log_{10} f_{O_2} = -11.75 \pm 0.10$, in excellent agreement with the anticipated f_{O_2} of the sensor runs, and therefore all reported pH_2 and f_{O_2} values are believed to be comparably accurate. The oxygen fugacity of each experimental charge was calculated using the f_{H_2} imposed by the Shaw membrane, the f_{H_2O} of the experimental charge, and H_2O formation constant from Robie and Hemingway (1995).

TABLE 1. Information about MagLiq series and SRD2 series

	T (°C)	P (MPa)	Duration (h)	pH_2 (bar)	log f_{O_2}	wt% Cl	wt% FeO[a]	Fe^{3+}/Fe^{Total}
MagLiq series								
MagLiq 5	950	150	333	2.56	–10.1	0.5	4.9 ± 0.13	ND
MagLiq6	950	150	333	2.56	–10.1	0.0	4.2 ± 0.18	ND
MagLiq7	950	130	214	0.86	–9.2	1.0	4.4 ± 0.19	ND
MagLiq8	950	130	214	0.86	–9.2	0.0	3.5 ± 0.13	ND
MagLiq Failed[b]	950	200	288	2.58	–9.0	0.6–0.75	3.4–5.2	ND
SRD2 series								
SRD2-2	950	130	138	6.41	–11	0.80	1.0 ± 0.07	0.33
SRD2-4	950	130	132	2.19	–10.1	0.80	1.3 ± 0.15	0.38
SRD2-9	950	130	214	0.85	–9.2	0.70	1.1 ± 0.15	0.42
SRD2-10	950	130	165	22.1	–11.9	0.70	0.6 ± 0.03	0.28

Notes: ND = not determined.

[a] The EPMA determined Fe contents of both the MagLiq series glasses and the SRD glasses are reported by convention as wt% "FeO". The locations of the EPMA analytical spots used to determine the Fe and Cl concentrations in these experiments were distributed randomly throughout the melt volume of the experimental charge from portion of the melt directly adjacent to the magnetite, to the distal portions of the melt at the opposite end of the charge. The values listed in the table are the mean of 15–20 spot analyses; the ± values following the mean are the 1σ standard deviation for the population of analyses.

[b] The values reported for the MagLiq Failed experiment are the ranges of Cl and Fe contents that were observed in the EPMA transect across the melt of the experimental charge. The approximate location of the analytical transect that produced these values is shown in Figure 1a.

EPMA AND XANES ANALYTICAL DETAILS

The EPMA-determined compositions of the equilibrium MagLiq glasses and the glasses from the magnetite-free SRD2 runs are given in Electronic Appendix I[1]. This appendix also contains detailed discussion of the EPMA and XANES analytical procedures, standards, and new XANES standard development.

RESULTS AND DISCUSSION

Using magnetite-dissolution experiments to examine potential Fe-Cl interactions in the melt

Perhaps the most direct way to observe potential Fe-Cl interactions in the melt is by examining the total Fe content (where total Fe content is equal to the sum of all Fe species present in the melt, i.e., Fe-O species and Fe-Cl species) of melts with various Cl contents in equilibrium with magnetite. Many of the MagLiq series experiments did not attain a homogenous Fe distribution in the melt; therefore these experiments were considered to be failed and will not be discussed in this section. The melts in four of the MagLiq series experiments appear to have achieved a uniform Fe distribution, and thus are believed to have attained a steady state. The results from only these experiments will be discussed in this section. The run conditions and the EMP determined Fe and Cl concentrations of the equilibrium MagLiq melts are presented in Table 1.

With these MagLiq series experiments we have attempted to isolate the effects of dissolved chlorine on the Fe^{total} content of the liquid required to support magnetite saturation. The equilibria governing magnetite dissolution illustrate how Cl may affect the EPMA measured iron content (which is reported with the EPMA data as "FeO") of the magnetite saturated melt. The magnetite dissolution reaction may be written as:

$$Fe_3O_4^{mag} = FeO^{melt} + 2FeO_{1.5}^{melt}$$

or alternatively expressed as a simple solubility product:

$$K_1 = (a FeO^{melt}) \times (a FeO_{1.5}^{melt})^2.$$

Additionally, fixing the f_{O_2} fixes the ratio of aFeO to aFeO$_{1.5}$ in melt via the homogenous redox reaction

$$FeO + 0.25O_2 = FeO_{1.5}$$
$$K_2 \cdot (f_{O_2})^{-0.25} = a FeO / a FeO_{1.5}.$$

From these reactions it is clear that perturbation of either aFeO or aFeO$_{1.5}$ due to changing f_{O_2} in the melt must be accompanied by either the dissolution or precipitation of magnetite to maintain equilibrium. However at fixed P, T, and f_{O_2}, the only way to perturb the total iron concentration in the melt is by altering the activity coefficients of either FeO or FeO$_{1.5}$ in the melt. The addition of Cl to the melt appears to produce this result. The results of the MagLiq experiments show that the addition of Cl to the melt is accompanied by a significant increase in the EPMA-determined total iron content of the quenched melt (see Table 1). For example, experiments MagLiq5 (Cl-bearing) and MagLiq6 (Cl-free) have EPMA-determined total Fe contents of

[1] Deposit item AM-15-75197, Electronic Appendix. Deposit items are stored on the MSA web site and available via the American Mineralogist Table of Contents. Find the article in the table of contents at GSW (ammin.geoscienceworld.org) or MSA (www.minsocam.org), and then click on the deposit link.

4.9 ± 0.13 and 4.2 ± 0.18 wt%, respectively (these values are reported as FeO in Table 1). The magnitude of the increase in Fe is not large, yet it is shown to be highly statistically significant when evaluated with a Student's t-test (the calculated two-tailed *P*-value for MagLiq 5 and 6 is <0.0001).

The observed increase in the iron concentration of the Cl-bearing experiments requires the presence of dissolved Cl to depress aFeO or aFeO$_{1.5}$ in the melt. Given what is known about potential Cl speciation in melts, there are two possible explanations for this behavior. The simplest explanation is that anionic Cl bonds with Fe in the melt to form stable Fe-Cl complexes, therefore lowering the activities of the Fe-O species in the melt. The second explanation requires the formation of Mg^{2+}-Cl, Ca^{2+}-Cl, or Na^{1+}-Cl in the melt; the presence of these complexes in some way fundamentally and indirectly changes aFeO and aFeO$_{1.5}$. It is important to note that the mechanisms presented above are not mutually exclusive, and that dissolved Cl is likely distributed among many competing divalent and monovalent cations. Unfortunately the magnetite dissolution experiments cannot be used to rigorously test the "direct Fe-Cl speciation" hypothesis vs. the "indirect complexing effect" hypothesis. The experiments described in the next two sections supplement the observations from the MagLiq experiments, further clarifying the chemical links between Fe and Cl in the melt.

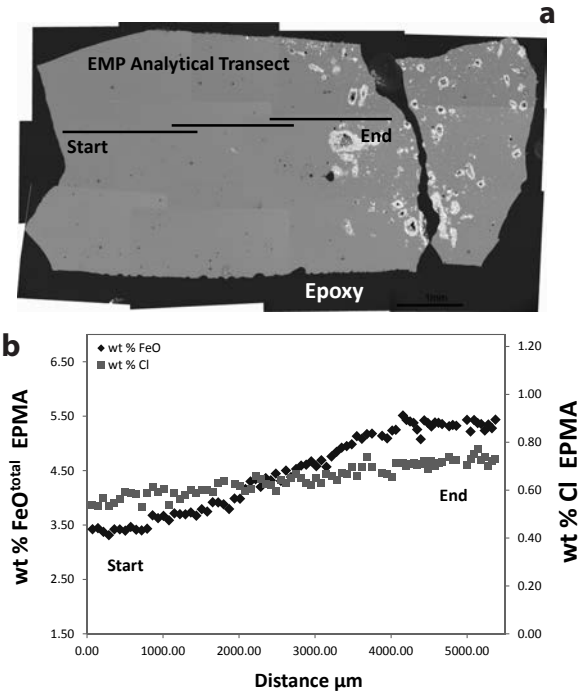

FIGURE 1. The image in **a** schematically shows the location of the EPMA analytical transect from the MagLiq Failed experiment (see Table 1). The experimental charge shown in the BSE image is comprised of two phases, glass (the light gray phase) and magnetite powder (the bright white phase). Image **b** shows a plot of FeO and Cl concentrations measured along the length of the transect that is shown in **a**. Distance 0.00 on the x-axis of the plot corresponds to the point labeled "Start" on the BSE image.

Evidence for Fe-Cl interaction

As discussed in the previous section, many of the magnetite-dissolution experiments failed to attain a uniform iron distribution in the melt. Although the failed experiments do not accurately depict the equilibrium iron content of the melt, they do capture a unique kinetic aspect of the magnetite-dissolution process that illuminates the chemical link between Fe and Cl in the melt. This section presents EPMA data from an analytical transect taken from the run products of one of the "failed" experiments. Figure 1a is a composite backscattered electron (BSE) image of the condensed products of one of the "disequilibrium" magnetite-dissolution experiments. Superimposed on this BSE image is the location of an EMP analytical transect across the quenched liquid. The compositional data plotted in Figure 1b show a thought-provoking relationship between the concentration profiles for FeO^{total} and Cl. As expected, the FeO^{total} content of the liquid monotonically decreases with distance from the interface of the magnetite-bearing and magnetite-free portions of the melt. The FeO^{total} content of the liquid nearest to the magnetite bearing melt appears to be a uniform ~5.5 wt% before decreasing to approximately 3.5 wt% in the distal portion of the glass.

We have interpreted this FeO^{total} distribution as a diffusion profile. In contrast to Fe, Cl appears to increase as the magnetite-melt interface is approached. The apparent redistribution of what was in the initial hours of the experiment a homogenous Cl concentration suggests that a Cl speciation reaction co-occurring with magnetite dissolution is causing this behavior. An example of such a speciation reaction involving Fe-Cl species is:

$$CaCl_2^{melt} + FeO^{melt} = FeCl_2^{melt} + CaO^{melt}$$

The addition of Fe to the melt from the magnetite dissolution results in the formation of Fe-Cl species. The Fe-enrichment of the melt causes in the stabilization of Fe-Cl species results in a melt with higher Cl solubility. It is the enhanced Cl solubility that is responsible for inducing a temporary Cl chemical potential in the melt. The existence of this gradient causes the observed "uphill" diffusive flux of Cl. If no interactions between melt components were occurring, the Cl content of the melt would simply decrease by dilution in the region adjacent to the magnetite-melt interface. Similar dissolution-diffusion arguments for melt speciation reactions have been invoked to describe homogenous alkali-Al speciation reactions in hydrous, haplogranitic melts (Acosta-Vigil et al. 2002, 2006). Using reasoning analogous to that presented in those studies, we conclude that the observed correlation between Fe and Cl concentrations suggests the occurrence of a Fe-Cl speciation reaction in the melt. The speciation reaction presented above should not be interpreted to mean that no other Cl species exist in the melt, but rather that Cl is distributed among the available cations in the melt in a manner that reflects the hierarchy of their relative stabilities. It is important to note that the results of the disequilibrium dissolution experiments cannot indicate which form of iron oxidation state—ferric or ferrous—is primarily involved in the proposed Cl-complexing reactions.

A causal link

In this section we focus primarily on the relationship between f_{O_2} and the response of the measured Fe valence in the melt. It is important to point out that XANES measurements themselves

can only yield information about the formal valence state of iron in the melt; therefore, the XANES-measured $Fe^{3+}/\Sigma Fe$ values of the glasses for the SRD experiments are given in Table 1 and have been plotted in Figure 2. The measured $Fe^{3+}/\Sigma Fe$ ranges from a low of 0.28 a high of 0.42. This relatively restricted range of values is remarkable, considering that the f_{O_2} varied in excess of three orders of magnitude in these experiments. The $Fe^{3+}/\Sigma Fe$ only increases by approximately 13%, as the experimentally imposed f_{O_2} increases from FMQ to FMQ + 3.2. To place this observation in context, the Kress and Carmichael (1991) model indicates that $Fe^{3+}/\Sigma Fe$ for the SRD melt should increase at nearly twice this rate in response to a 3.2 log unit increase in f_{O_2}. The relationship between $Fe^{3+}/\Sigma Fe$ and f_{O_2} that we have observed for the chlorinated SRD melts is unique. No previous studies have yielded similar results with respect to the *slope* of the ferric-ferrous ratio as a function of f_{O_2}. In all previous studies of hydrous melts, none of which contained Cl, the observed relationship between $Fe^{3+}/\Sigma Fe$ and f_{O_2} has been consistent with the apparent reaction stoichiometry as either defined by the Kress and Carmichael (1991) equation, or the theoretical reaction stoichiometry (Jayasuriya et al. 2004). The Fe valence data from the SRD experiments suggest that the addition of Cl to the melt fundamentally changes the relationship between Fe valence and f_{O_2}, as the rate at which the measured Fe^{3+} abundance increases in the melt appears to be damped.

The relationship between $Fe^{3+}/\Sigma Fe$ and f_{O_2} observed in the SRD experiments may be interpreted in several different ways. Here we present two possible interpretations of the Fe^{3+}/Fe data: (1) the formation of Fe^{2+}-Cl species partially decouples the measured formal valence ratio from the imposed experimental f_{O_2}, and (2) the changes in Cl-speciation in the melt co-occurring with Fe oxidation alter the activity ratio of FeO and $FeO_{1.5}$ in the melt. It is important to note that these interpretations are not mutually exclusive, and that the mechanisms proposed may both significantly affect the equilibrium $Fe^{3+}/\Sigma Fe$.

In the first interpretation, the addition of Cl to the melt results in the formation of Fe^{2+}-Cl species. If such a species exists in the melt, then the denominator of the $Fe^{3+}/\Sigma Fe$ ratio is partially controlled by the abundance of the Fe^{2+}-Cl species in the melt. As f_{O_2} in the melt is increased, the $FeO_{1.5}/FeO$ ratio may indeed still increase following the expected stoichiometry, however, the persistent presence of Fe^{2+}-Cl species in the higher f_{O_2} experiments acts to suppress the expected increase in the measured $Fe^{3+}/\Sigma Fe$ with f_{O_2}. Realistically, this simplified explanation may be complicated by homogenous Cl speciation reactions, as the abundance of FeCl species may be, in part, linked to the activity of FeO in a complex way.

It is also possible to rationalize the observed Fe^{3+}/Fe^{2+} vs. f_{O_2} trend by considering how the distribution of Cl species in the melt changes as a function of f_{O_2}. The preponderance of the available Cl solubility and phase equilibrium studies suggest that many different cations are ultimately involved in forming Cl species within the melt. Therefore it follows that the Cl content of the melt is not simply determined by a single canonical Cl species, but instead it is a reflection of a hierarchical distribution, where Cl is appropriated among the various competing cations according to the relative stabilities of their Cl complexes. The results of Webster and DeVivo (2002) indicate that the relative stability

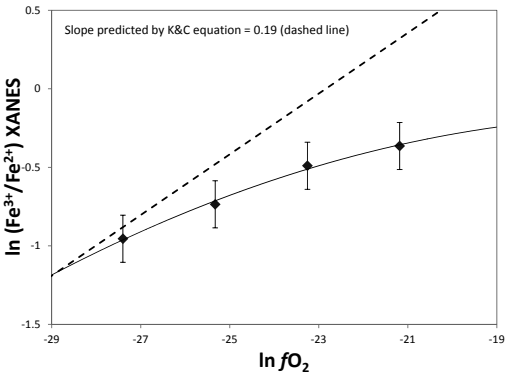

FIGURE 2. An ln-ln plot of the XANES measured Fe^{3+}/Fe^{2+} ratios of the SRD Series experiments vs. the experimental f_{O_2} values. The dashed line represents the slope of the homogenous ferric-ferrous equilibrium as predicted by the Kress and Carmichael equation (1991), which is shown as a frame of reference. The deviation from the predicted slope systematically becomes larger as f_{O_2} increases.

of Cl species follows a general pattern where Ca^{2+}-Cl = Mg^{2+}-Cl > Fe^{2+}-Cl >> Na^{1+}-Cl > K^{1+}-Cl. As such the distribution of Cl species in the melt can be described as a series of homogenous speciation reactions:

$$FeCl_2 + Na_2O = FeO + 2NaCl$$
$$FeCl_2 + CaO = FeO + CaCl_2$$
$$FeCl_2 + K_2O = FeO + 2KCl$$

At fixed melt composition, temperature, pressure, and f_{O_2}, the distribution of Cl species is fully defined by a combination of the appropriate homogenous speciation equilibria. It therefore follows that under more oxidized conditions the apparent speciation behavior of Cl should change substantially. In the case of our experiments, it appears that increasing f_{O_2} disturbs the equilibrium distribution of Cl in the melt by decreasing the availability of Fe^{2+} to form $FeCl_2$ species. If the Cl concentration of the melt remains nearly constant, as it does in our experiments, then the decreased FeO content of the melt must be accompanied by a concomitant shift in the Cl species distribution. Increasing f_{O_2} effectively redistributes some Cl that was formerly bonded to Fe^{2+} to form Cl complexes with the alkalis and alkaline earth cations. In other words, at higher f_{O_2}, the Cl speciation shifts to favor the formation of Na-Cl or Ca-Cl species over Fe^{2+}-Cl species. The result of this process is an effective depression of the $Na_2O/NaCl$, K_2O/KCl, and $CaO/CaCl_2$ ratios in the melt.

Redox-induced changes in Cl speciation may also be responsible for suppressing the formation of $FeO_{1.5}$ with increasing experimental f_{O_2}. Increased abundances of $CaCl_2$, NaCl, and KCl in the melt appear to decrease the "effective" alkalinity of the melt, thus depressing the equilibrium $Fe^{3+}/\Sigma Fe$. The relationship between melt alkalinity and $Fe^{3+}/\Sigma Fe$ has been well documented by numerous studies (Mysen et al. 1980; Sack et al. 1980; Kress and Carmichael 1991). These studies have unanimously shown that increasing concentrations of K_2O, Na_2O, and CaO cause an increase in the equilibrium $Fe^{3+}/\Sigma Fe$ at constant f_{O_2}. This effect has been attributed to the structural role of these cations as possible charge compensators for $^{IV}Fe^{3+}$ in the melt by forming species such as $NaFe^{3+}O_2$ (Mysen et al. 1980). Our data suggest

chlorinated alkalis may not effectively act as charge compensators for $^{IV}Fe^{3+}$ in bonding configurations such as Fe^{3+}-Cl-Na^{1+}. Alternatively, the effects of changing Cl-speciation on the melt alkalinity may be understood in terms of the link between polymerization state and optical basicity of a melt and its equilibrium $Fe^{3+}/\Sigma Fe$ (Ottonello et al. 2001). In the case of our experiments, formation of alkali- and alkaline earth-Cl complexes may decrease the NBO/T (non-bridging oxygen per tetrahedral cation) and basicity of the melt, thereby enhancing the stability of $Fe^{2+}O$ species in the melt. The effects of Cl on the NBO/T of natural aluminosilicate melts may in fact be significantly more complex than the simple relationships described above, therefore the potential importance of the role of Cl in altering the $Fe^{3+}/\Sigma Fe$ via changing the melt NBO/T is still an open question.

Implications

It has been proposed that onset of magnetite crystallization plays a critical role in modulating the onset of Fe-Cu sulfide saturation in arc magmas (Jenner et al. 2010). In this way, the suppressing effect of Cl on magnetite saturation may help keep the sulfide in Cl-enriched arc magmas undersaturated until an exsolved volatile phase has removed a significant quantity of Cl from the melt. From the perspective of ore deposit formation, the timing of sulfide saturation controls the total metal budget of the causative magma; it is therefore critical that the role of Cl is understood in the context of how it alters the stability of ferric-iron-bearing minerals.

Additionally, the equilibrium $Fe^{3+}/\Sigma Fe$ of the melt is significantly affected by the presence of Cl. This relationship may be the effect of two different but complementary mechanisms—the formation of ferrous-chloride complexes in the melt as well as the formation of alkali chloride species. In either case, the removal of Cl from the melt will result in the stabilization of $FeO_{1.5}$ at the expense of FeO, provided that the system is open with respect to oxygen (or H_2, as the case may be). Though this initial work hints at the important relationship between Fe and Cl in felsic-intermediate melts, much more work is required to fully appreciate and understand the extent to which Cl may alter the fundamental redox behavior and phase equilibria of arc magmas.

Acknowledgments

A.S.B. thanks the AMNH for providing the Kalbfleisch Postdoctoral Fellowship and additional funding, without which this work would not have been possible. We thank M. Newville at APS for his assistance with the acquisition of the XANES spectra and the subsequent data processing, M.D. Dyar and E. Breves are thanked for their assistance in the acquisition and interpretation of the Mössbauer data. We are also indebted to D. Ebel and M. Wilke for providing valuable discussion and informal reviews of an early version of this manuscript. E. Cottrell is thanked for graciously providing the set of rhyolitic glass standards. AE Ian Swainson is thanked for his patience and editorial efforts. Katy Evans and two anonymous reviewers are also thanked for their constructive comments and criticisms, which greatly benefited the final manuscript. Portions of this work were performed at GeoSoilEnviroCARS (Sector 13), Advanced Photon Source (APS), Argonne National Laboratory. GeoSoilEnviroCARS is supported by the National Science Foundation–Earth Sciences (EAR-1128799) and Department of Energy–Geosciences (DE-447 FG02-94ER14466). Use of the Advanced Photon Source was supported by the U.S. Department of Energy, Office of Science, 448 Office of Basic Energy Sciences, under Contract No. DE-AC02-06CH113.

References cited

Acosta-Vigil, A., London, D., Dewers, T., and Morgan, G.B. (2002) Dissolution of corundum and andalusite in H_2O-saturated haplogranitic melts at 800°C and 200 MPa: constraints on diffusivities and the generation of peraluminous melts Journal of Petrology, 43, 1885–1908.

——— (2006) Dissolution of quartz, albite, and orthoclase in H_2O-saturated haplogranitic melt at 800 °C and 200 MPa: diffusive transport properties of granitic melts at crustal anatectic conditions Journal of Petrology, 47, 231–254.

Baker, L.L., and Rutherford, M.J. (1996) The effect of dissolved water on the oxidation state of silicic melts. Geochimica et Cosmochimica Acta, 60, 2179–2187.

Bell, A.S., and Simon, A. (2011) Experimental evidence for the alternation of $Fe^{3+}/\Sigma Fe$ of silicate melt caused by chlorine rich aqueous volatiles. Geology, 39, 499–502.

Borisov, A., and McCammon, C. (2010) The effect of silica on ferric/ferrous ratios in silicate melts: An experimental investigation using Mössbauer spectroscopy. American Mineralogist, 95, 545–555.

Carroll, M.R., and Webster, J.D. (1994) Solubilities of sulfur, noble gases, nitrogen, chlorine, and fluorine in magmas. In M.R. Carroll and J.R. Holloway, Eds., Volatiles in Magmas, 30, 231–279. Reviews in Mineralogy, Mineralogical Society of America, Chantilly, Virginia.

Dingwell, D.B., and Hess, K-U. (1998) Melt viscosities in the system Na–Fe–Si–O–F–Cl: Contrasting effects of F and Cl in alkaline melts American Mineralogist, 83, 1016–1021.

Evans, K.A., Mavrogenes, J.A., O'Neill, H.S., Keller, N.S., and Jang, L.Y. (2008) A preliminary investigation of chlorine XANES in silicate glasses. Geochemistry, Geophysics, Geosystems, 9, Q10003.

Filiberto, J., and Treiman, A.H. (2009) The effect of chlorine on the liquidus of basalt: First results and implications for basalt genesis on Mars and Earth. Chemical Geology, 263, 60–68.

Filiberto, J., Dasgupta, R., Gross, J., and Treiman, A. (2014) Effect of chlorine on near-liquidus phase equilibria of an Fe–Mg-rich tholeiitic basalt. Contributions to Mineralogy and Petrology, 168, 1–13.

Gaillard, F., Scaillet, B., Pichavant, M., and Bény, J.-M. (2001) The effect of water and f_{O_2} on the ferric-ferrous ratio of silicic melts. Chemical Geology, 174, 255–273.

Jayasuriya, K.D., O'Neill, H.St.C., Berry, A., and Campbell, S.J. (2004) A Mössbauer study of the oxidation state of Fe in silicate melts. American Mineralogist, 89, 1597–1609.

Jenner, F.E., O'Neill, H.St.C., Arculus, R.J., and Mavrogenes, J.A. (2010) The magnetite crisis in the evolution of arc-related magmas and the initial concentration of Au, Ag and Cu. Journal of Petrology, 51, 2445–2464.

Killinc, A., Carmichael, I.S.E., Rivers, M.L., and Sack, R.O. (1983) The ferric ferrous ratio of natural silicate liquids equilibrated in air. Contributions to Mineralogy and Petrology, 83, 136–140.

Kress, V.C., and Carmichael, I.S.E. (1991) The compressibility of silicate liquids containing Fe_2O_3 and the effect of composition, temperature, oxygen fugacity and pressure on their redox states. Contributions to Mineralogy and Petrology, 108, 82–92.

Moore, G., Righter, K., and Carmichael, I.S.E. (1995) The effect of dissolved water on the oxidation state of iron in natural silicate liquids. Contributions to Mineralogy and Petrology, 120, 170–179.

Moretti, R. (2005) Polymerisation, basicity, oxidation state and their role in ionic modelling of silicate melts. Annals of Geophysics, 48, 583–608.

Mysen, B., Seifert, F., and Virgo, D. (1980) Structure and redox equilibria of iron bearing silicate melts. American Mineralogist, 65, 867–884.

Ottonello, G., Moretti, R., Marini, L., and Vetuschi Zuccolini, M. (2001) Oxidation state of iron in silicate glasses and melts: a thermochemical model. Chemical Geology, 174, 157–179.

Robie, R.A., and Hemingway, B.S. (1995) Thermodynamic properties of minerals and related substances at 298.15 K and 1 bar (10^5 Pascals) pressure and at higher temperatures. U.S. Geological Survey Bulletin, No. 2131, 461 pp.

Sack, R.O., Carmichael, I.S.E., Rivers, M.L., and Ghiorso, M.L. (1980) Ferric-ferrous equilibria in natural silicate liquids at 1 bar. Contributions to Mineralogy and Petrology, 75, 369–376.

Tangeman, J.A., Lange, R.A., and Forman, L. (2001) Ferric-ferrous equilibria in K_2O-FeO-Fe_2O_3-SiO_2 melts. Geochimica et Cosmochimica Acta, 65, 1809–1819.

Taylor, J.R., Wall, V.J., and Pownceby, M.I. (1992) The calibration and application of accurate redox sensors. American Mineralogist, 77, 284–295.

Wallace, P.J. (2005) Volatiles in subduction zone magmas: concentrations and fluxes based on melt inclusion and volcanic gas data. Journal of Volcanology and Geothermal Research, 140, 217–240.

Webb, S.L., Bramley, M.J., and Wheeler, A.J. (2014) Rheology and the Fe^{3+}–chlorine reaction in basaltic melts. Chemical Geology, 366, 24–31.

Webster, J.D., and De Vivo, B. (2002) Experimental and modeled solubilities of chlorine in aluminosilicate melts, consequences of magma evolution, and implications for exsolution of hydrous chloride melt at Mt. Somma-Vesuvius. American Mineralogist, 87, 1046–1061.

Webster, J.D., Vetere F, Botcharnikov, R.E., Goldoff, B., McBirney A., and Doherty, A.L. (2015) Experimental and modeled chlorine solubilities in aluminosilicate melts at 1 to 7000 bars and 700 to 1250 °C: Applications to magmas of Augustine Volcano, Alaska. American Mineralogist, 100, 522–535.

Wilke, M. (2005) Fe in magma: an overview. Annals of Geophysics, 48, 609–617.

Wilke, M., Behrens, H., Burkhard, D.J.M., and Rossano, S. (2002) The oxidation state of iron in silicic melt at 500 MPa water pressure. Chemical Geology, 189, 55–67.

Zimova, M., and Webb, S. (2006) The effect of chlorine on the viscosity of Na_2O–Fe_2O_3–Al_2O_3–SiO_2 melts. American Mineralogist, 91, 344–352.

Manuscript received September 19, 2014
Manuscript accepted February 10, 2015
Manuscript handled by Ian Swainson